

# First real-time detection of surface dust in a tokamak<sup>a)</sup>

C. H. Skinner,<sup>1,b)</sup> B. Rais,<sup>2</sup> A. L. Roquemore,<sup>1</sup> H. W. Kugel,<sup>1</sup> R. Marsala,<sup>1</sup> and T. Provost<sup>1</sup><sup>1</sup>*Princeton Plasma Physics Laboratory, Princeton, New Jersey 08543, USA*<sup>2</sup>*Université de Provence, Aix-Marseille 13003, France*(Presented 19 May 2010; received 14 May 2010; accepted 7 June 2010;  
published online 1 October 2010)

The first real-time detection of surface dust inside a tokamak was made using an electrostatic dust detector. A fine grid of interlocking circuit traces was installed in the NSTX vessel and biased to 50 V. Impinging dust particles created a temporary short circuit and the resulting current pulse was recorded by counting electronics. The techniques used to increase the detector sensitivity by a factor of  $\times 10\,000$  to match NSTX dust levels while suppressing electrical pickup are presented. The results were validated by comparison to laboratory measurements, by the null signal from a covered detector that was only sensitive to pickup, and by the dramatic increase in signal when Li particles were introduced for wall conditioning purposes. © 2010 American Institute of Physics.

[doi:[10.1063/1.3464465](https://doi.org/10.1063/1.3464465)]

## I. INTRODUCTION

High levels of dust are expected in next step fusion devices because of the intense plasma-wall interactions and long pulse duration.<sup>1</sup> The dust can be radioactive from tritium or activated tungsten, toxic, and/or chemically reactive with steam or air and the accumulation of dust will have operational and potential safety impacts in four areas. To limit the radiological source term in case of accidental release to the environment the quantity of dust in ITER will be maintained below 1000 kg.<sup>2</sup> An administrative limit of 670 kg is envisioned to take account of measurement uncertainties. Second, to limit the potential explosion hazard in case a coolant leak and simultaneous air ingress result in hydrogen generation from chemical reactions between dust on hot surfaces and steam/water, the quantity of dust on hot surfaces will be maintained below 6 kg of C and 6 kg of Be, or if C is absent, 11 kg of Be and 230 kg of W. Third, dust transport to the core plasma will raise impurity concentrations, degrade fusion performance, and may cause disruptions. Fourth, dust may coat diagnostic mirrors necessary to monitor plasma operations and compromise their performance. The tolerable amount of dust for the last two issues is not known. Clearly dust detection and dust removal techniques will be vital to the operation of ITER and future fusion reactors.

The ITER strategy<sup>2</sup> includes indirect measurement of dust generation via measurements of the erosion of plasma facing components. Initially 100% of the erosion products will be conservatively assumed to be dust. Dust will be removed from the vessel by vacuum cleaning during the maintenance periods planned for divertor replacement and this is expected to be sufficient to maintain the global dust inven-

tory below the 670 kg limit. Electrostatic traveling waves have been proposed to prevent the accumulation of dust on photovoltaic cells in space missions<sup>3</sup> and initial results with a view applying this technology to dust removal in tokamaks are reported in Refs. 4 and 5. Direct local measurements of dust are envisioned to provide information on dust generation on a pulse-by-pulse basis with a measurement requirement of 20% relative and 50% absolute accuracy. However dust measurement techniques are still in their infancy, especially for dust on hot surfaces and to date no real-time measurements of surface dust in tokamaks have been reported.

A capacitive diaphragm pressure gauge that is adapted for use as a dust microbalance has been proposed for local dust measurements and a prototype with a sensitivity of 0.5 mg/cm<sup>2</sup> has been tested in the laboratory.<sup>6</sup> These devices rely on the long term measurement of nanometer-scale mechanical displacements and significant challenges remain to maintain thermal and mechanical stability in the face of ELMs and disruptions in the ITER divertor. An alternative technique relies on electrostatic effects and we report on the first real-time measurement of surface dust in an operating tokamak using this technique. The physics of dust in plasmas has been reviewed in Ref. 7 and previous work on dust diagnostic techniques has been recently reviewed in Refs. 8 and 9.

## II. LABORATORY DEVELOPMENT OF AN ELECTROSTATIC DUST DETECTOR

The device is designed to detect dust particles settling on a remote surface. In the present embodiment two closely interlocking combs of copper traces on a circuit board are biased at 30–50 V (Fig. 1). When a conductive dust particle settles on this surface a miniature spark is generated creating a transient short circuit and the resulting current pulse is detected electronically. At the same time the heat generated by the current vaporizes at least part of the particle causing it to rocket off the surface or vaporize. This restores the open

<sup>a)</sup> Contributed paper, published as part of the Proceedings of the 18th Topical Conference on High-Temperature Plasma Diagnostics, Wildwood, New Jersey, May 2010.

<sup>b)</sup> Author to whom correspondence should be addressed. Electronic mail: cskinner@pppl.gov.

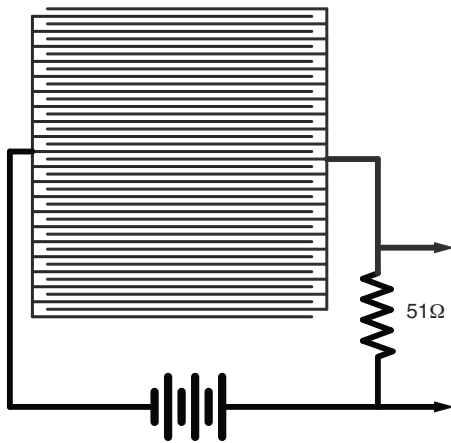


FIG. 1. Schematic of dust detector (not to scale) showing interlocking combs of traces. Dust impinging on the traces causes a short circuit and a voltage signal is generated across the 51  $\Omega$  resistor.

circuit, resetting the detector for the next dust particle. Initial laboratory tests in air and vacuum using standard nuclear counting electronics (single channel analyzer) showed a correlation between the signal and amount of dust and, in the early work, a threshold sensitivity of  $\sim 50 \mu\text{g}/\text{cm}^2$  in air at a trace spacing of 127  $\mu\text{m}$  was measured.<sup>10,11</sup> However this sensitivity is approximately four orders of magnitude above that needed to detect dust falling during one pulse in contemporary tokamaks so further development was needed.

An increase in sensitivity [expressed in counts/areal density (counts/ $\text{g}/\text{cm}^2$ )], of more than an order of magnitude was obtained with ultrafine traces with 25  $\mu\text{m}$  separation.<sup>12</sup> The carbon test particles used in the initial experiments ranged from 1 to 500  $\mu\text{m}$  in size with most of the particles being close to 1  $\mu\text{m}$ . The sensitivity was measured with particles in different size ranges to determine if the detector response was predominately from the relatively few particles with size sufficient to bridge the gap between traces or from the many particles smaller than the gap size. It was found that the response was the highest for the finest particles. This is a favorable property for tokamak dust which is predominately of micron scale. The number density of incident particles (whatever their size) was the dominant factor in the response. Qualitative information on the size of the particles was also apparent as larger particles generated longer current pulses.

Typically open circuit conditions are rapidly restored indicating that the dust particles have been removed from the circuit board. The fate of the dust particles was tracked by measurements of mass gain/loss. Heating by the current pulse caused up to 90% of the particles to be ejected from the circuit board.<sup>13</sup> Further improvements in detector sensitivity were obtained by increasing the area of the detector from  $12.7 \times 12.3$  to  $50.8 \times 50.8 \text{ mm}^2$ .<sup>14</sup> A high sensitivity balance was used to measure microgram levels of dust delivered to the detector and the response was quite linear down to the lowest mass indicating that single particles were sufficient to cause breakdown. To bridge the remaining gap in detector sensitivity compared to the dust levels in present tokamaks, the detection electronics were modified.<sup>15</sup> A low pass filter used for signal conditioning was removed, and the single

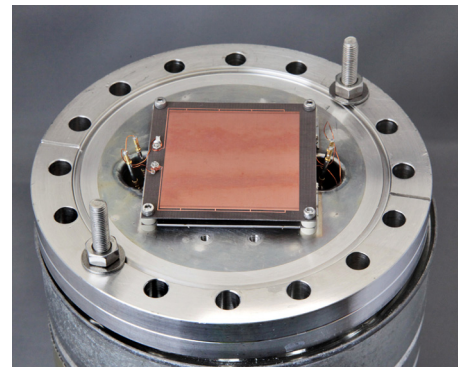


FIG. 2. (Color online) Dust detector before installation in NSTX.

channel analyzer voltage threshold was lowered. The sensitivity further increased by a factor of 2 when the bias voltage was decreased from 50 to 25 V, possibly because multiple pulses were generated from the same particle as it was not promptly ejected from the circuit board. Altogether these changes in the electronics increased the sensitivity (counts/ $\text{ng}/\text{cm}^2$ ) a further factor of  $\times 120$  bringing it to the level required.

### III. DUST DETECTION ON NSTX

The National Spherical Torus Experiment (NSTX) is a low aspect ratio tokamak aimed at establishing the physics basis for next-step devices such as a plasma facing component test facility and to support ITER.<sup>16</sup> The trajectories of dust particles in the plasma have been recorded by stereoscopic fast cameras and compared to modeling.<sup>17</sup> Dust samples were also taken with a vacuum pump and filter attachment from several locations in the NSTX vessel during a maintenance period and the average count median diameter of this dust was found to be 3.27  $\mu\text{m}$ .<sup>18</sup> Surface dust levels at the bottom of the vessel were measured by weighing the dust collected on a glass slide over 1249 discharges resulting in an average dust level of 5.6  $\text{ng}/\text{cm}^2$  discharge.<sup>13</sup> Particles that had accumulated on a viewport at the bottom of the vessel after 520 discharges were also examined with a digital optical microscope.<sup>11</sup> The particle density was 313 500 particles/ $\text{cm}^2$ , with a count median diameter 2.06  $\mu\text{m}$ , similar to values found in other tokamaks. This direct viewing method gives a direct measure of the particle areal density and has the advantage that the dust is not disturbed by a dust collection technique.

#### A. Detector configuration

Two 50.8 mm electrostatic detectors were mounted on a 15 cm conflat flange (Fig. 2). To distinguish the dust signal from electrical pickup, two circuit boards were used in NSTX, one above the other. The lower board was covered with mica to prevent any dust from reaching it and was therefore only sensitive to electrical pickup. A stainless steel wire mesh with pore size  $90 \times 90 \mu\text{m}^2$  covered both detectors and prevented large debris and fibers from settling on the detector.

The detector was installed at a vertical port 60 cm below a 5 cm wide radial slot located between the outer divertor

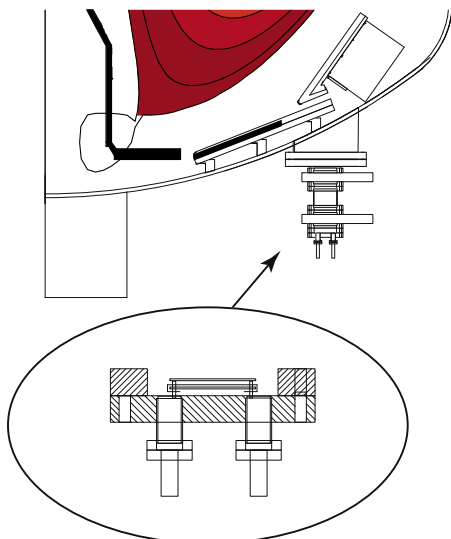


FIG. 3. (Color online) Poloidal cross section of NSTX vessel with close up of dust detector.

and inner passive plate at Bay C (Fig. 3). This was isolated from the vacuum vessel by a double gate valve (two gate valves were necessary as falling dust could interfere with the valve seal). The assembly was wrapped in heater tape and baked to a temperature of  $65\text{ }^{\circ}\text{C}$  for 36 h to outgas volatile molecules from the components before the gate valves were opened to the NSTX vacuum. Triaxial cables 30 m long connected the detectors to the 50 V supply and detection electronics. Intershot helium glow discharges are sometimes performed on NSTX for wall conditioning purposes. To prevent any potential interactions the detector bias voltage was automatically disconnected during periods of glow.

The changes described in Sec. II increased the sensitivity by four orders of magnitude; however this caused some initial problems in the tokamak environment. With the bias set to 30 V for maximal sensitivity the dust particles were not always cleared from the detector and a permanent short could occur. In some cases this could be cleared by cycling the bias voltage on and off many times, but this was inconvenient. The voltage was increased back to 50 V which avoided this problem. A second issue was in confidently distinguishing dust signals from electrical pick-up in the tokamak electrical environment with high power rf and switched power amplifiers in the vicinity.

## B. Detector electronics

A differential detection electronics circuit was implemented to address this and is shown schematically in Fig. 4. The detector is biased to 50 V through  $25\ \Omega$  resistors rated at 44 W, four times the maximum power that can be supplied in case of a complete short circuit. The balanced inputs from the detector are first attenuated by a factor of 10 using a precision differential attenuator (a), and input to an Analog Devices ([www.analog.com](http://www.analog.com)) 10 MHz instrumentation amplifier, AD8250ARMZ, with a gain of unity (b). The amplifier is followed by a low pass filter that is switchable between 200 ns and  $5.6\ \mu\text{s}$  (c) (set to 200 ns for this work) and a comparator (d) that compares the signal to an adjustable ref-

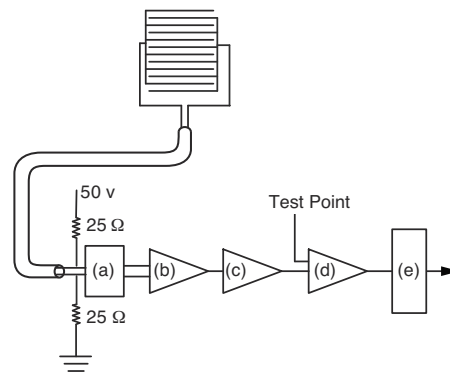


FIG. 4. Schematic of differential detection electronics. See text for explanation of components.

erence trip point. This is currently set to 4.58 V and corresponds to a resistance between the detector traces of less than  $480\ \Omega$ . When the signal is lower than the trip point a 5 V output pulse is fed to a nonretriggerable one-shot that outputs a  $1\ \mu\text{s}$  pulse to a Bi Ra 911 latching scalar with a 256 K memory module. Data from this are acquired at 1 kHz from a period of  $-10$  to 55 s with respect to the initiation of the plasma. Two identical and independent electronics channels were used for the two detectors.

## C. Detector calibration

The laboratory dust source<sup>15</sup> was taken to the NSTX test cell to characterize the time history of a known dust signal. A typical signal from dust released by a one-time event (knock) is shown in Fig. 5 (for this measurement an earlier, nondifferential version of the detection electronics<sup>15</sup> was used). The signal extends over 10 s or more as the particles interact with the circuit board. The detector was absolutely calibrated in the laboratory. Carbon particles were scraped from a spare NSTX ATJ graphite tile and the particle size was measured by microscopic imaging and particle size analysis as described in Ref. 12. The count median diameter was determined to be  $2.14\ \mu\text{m}$ , similar to the particles from NSTX. A few micrograms of carbon particles were dropped on the detector in air and vacuum and the response of the differential detection electronics was recorded. Data from a 50.8 mm

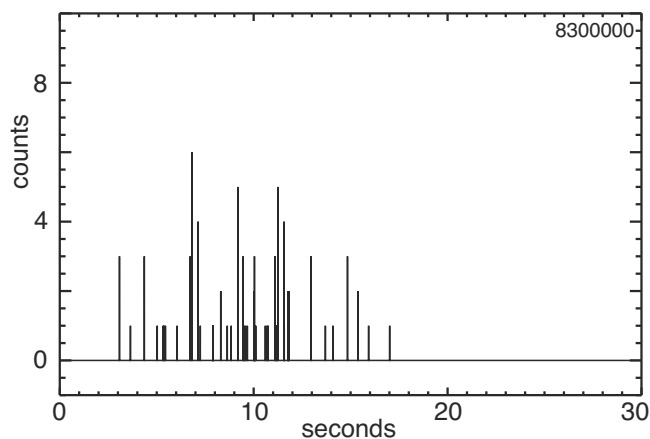


FIG. 5. Signal generated by laboratory dust source incident on detector as recorded by the NSTX data acquisition system.

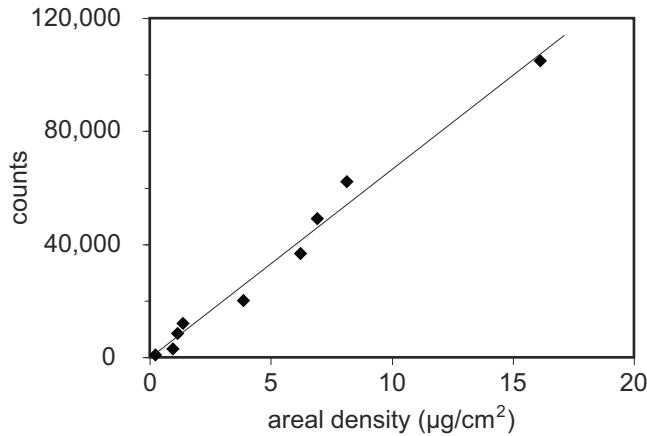


FIG. 6. Response of 50.8 mm detector to carbon dust in vacuum, using a 50 V bias, differential counting electronics, and mesh cover. The line is a linear fit to the data

detector covered with the 90  $\mu\text{m}$  pore mesh are shown in Fig. 6. The threshold sensitivity of the 50.8 mm detector to carbon particles in vacuum is 0.15  $\text{ng}/\text{cm}^2/\text{count}$ . These data include some counts triggered by residual dust on the detector after the dust source was removed. The detector was cleaned with compressed gas in between each measurement. In NSTX the response may be somewhat influenced by residual dust and a gas puffing system is under development. The equipment was moved to an argon filled glove box to repeat the calibration with 40  $\mu\text{m}$  diameter lithium particles.<sup>19</sup> These particles are used for NSTX wall conditioning (see below) and the argon was necessary to minimize the oxidation of the lithium particles during handling. A 12 mm detector was used with the lithium particles and the sensitivity in vacuum without mesh cover was measured to be 14.5  $\text{ng}/\text{cm}^2/\text{count}$ . The lower sensitivity for the larger Li particles is consistent with the results of Ref. 12. A detailed account of the calibration is given in Ref. 20.

#### IV. FIRST RESULTS ON NSTX

The first day of detector operation with NSTX discharges showed a signal up to 70 counts on the upper (open) detector (Ch. 1) with zero (or in one case 2) counts on the mica covered detector (Ch. 2). The time history of the Ch. 1 signal [Fig. 7(a)] was similar to that obtained with the laboratory dust source. The lack of signal on Ch. 2 [Fig. 7(b)] is strong evidence that the Ch. 1 signals are due to dust. The history of the total number of counts versus shot number for July and August 2009 is shown in Fig. 8. The signal (pickup) on the covered detector is zero (not plotable on the log plot), or a few counts in less than 10% of discharges. On two days the tokamak was electrically reconfigured for coaxial helicity injection (CHI) and up to 17 counts of pickup was observed for a few CHI discharges.

The conspicuous two-order-of-magnitude increase in dust signal starting with shot 135832 is correlated with the operation of a lithium aerosol at Bay C upper port (directly above the dust detector). This drops lithium particles<sup>19</sup> into the plasma for wall conditioning purposes.<sup>21</sup> A second large increase in the dust signal is coincident with the second operation of the Li aerosol on shot 136150. The exact correla-

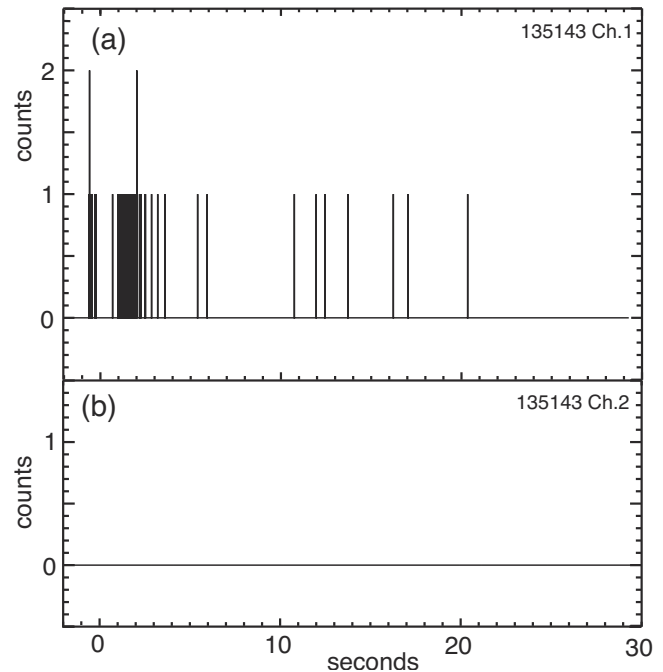


FIG. 7. (a) Dust signal; there is a total of 64 counts from dust. (b) The simultaneous null signal from the covered detector.

tion of aerosol operation with the increase in dust signal is compelling evidence that the dust signals are due to particles impinging on the detector. The signal markedly decreases after the aerosol ceases operation, but does not return down

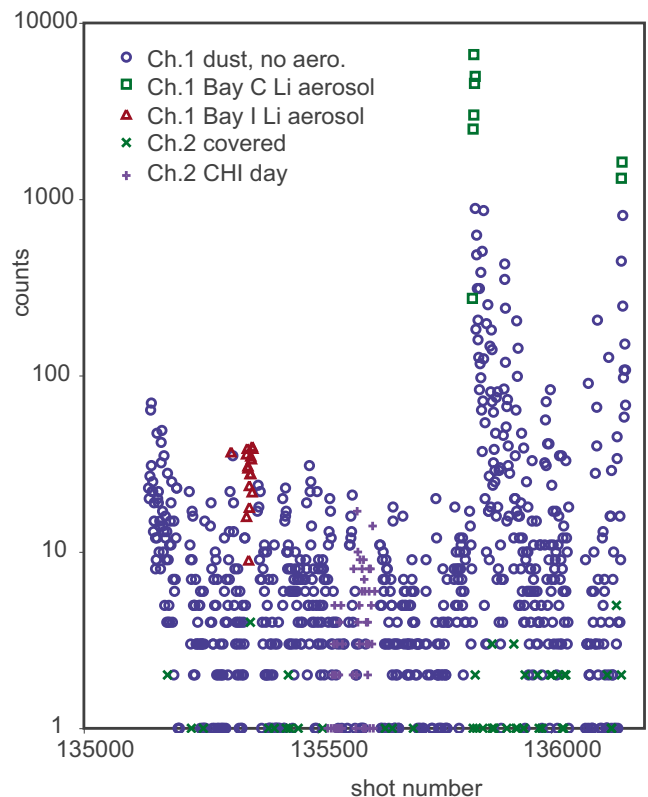


FIG. 8. (Color online) (a) Time history of channel 1 (open detector) and channel 2 (covered detector) signals vs shot number over July and August 2009. The points where the Li aerosol was operated are distinguished in the legend. Note the two-order-of-magnitude increase in signal with the operation of the Bay C Li aerosol.



to the original level indicating that a few percent of the particles may remain on the detector (consistent with laboratory results).<sup>13</sup> Some lithium particles were visible on the detector after it was retrieved from the vessel at the end of the campaign. In future work a helium gas puffing system such as described in Ref. 5 will be added to periodically clear residual particles remaining on the detector.

In summary, we report the first real-time detection of surface dust inside a tokamak. Details of the correlation of the dust signals with plasma events will be reported separately. We note that development work remains to make these detectors compatible with the harsh ITER in-vessel environment. The detector will need to be fabricated from radiation resistant materials and operate reliably for long periods without maintenance. A ruggedized detector is needed to detect tungsten dust. However the dust levels of concern in ITER are much higher than the levels in existing tokamaks. 1 kg of dust spread uniformly over the ITER horizontal cross section corresponds to 0.60 mg/cm<sup>2</sup> so a less sensitive detector with thicker, more rugged traces would be appropriate.

## ACKNOWLEDGMENTS

The authors would like to thank National Undergraduate fellows A. Bader, D. Boyle, A. Campos, C. Parker, R. Hensley, and C. Voinier for previous work and C. Bunting, M. Cropper, and T. Holoman for technical assistance. We are indebted to D. Mansfield for assistance in handling the lithium particles. This work was funded by the U.S. DOE Grant No. DE AC02-09CH11466.

- <sup>1</sup>G. Federici, C. H. Skinner, J. N. Brooks, J. P. Coad, C. Grisolia, A. A. Haasz, A. Hassanein, V. Philipps, C. S. Pitcher, J. Roth, W. R. Wampler, and D. G. Whyte, *Nucl. Fusion* **41**, 1967 (2001).
- <sup>2</sup>S. Rosanvallon, C. Grisolia, P. Andrew, S. Ciattaglia, P. Delaporte, D. Douai, D. Garnier, E. Gauthier, W. Gulden, S. H. Hong, S. Pitcher, L. Rodriguez, N. Taylor, A. Tesini, S. Vartanian, A. Vetry, and M. Wykes, *J. Nucl. Mater.* **390–391**, 57 (2009).
- <sup>3</sup>C. I. Calle, J. L. McFall, C. R. Buhler, S. J. Snyder, E. E. Arens, A. Chen, M. L. Ritz, J. S. Clements, C. R. Fortier, and S. Trigwell, Proceedings of the ESA Annual Meeting on Electrostatics, 2008, p. 1.
- <sup>4</sup>C. H. Skinner, A. Campos, H. Kugel, J. Leisure, A. L. Roquemore, and S. Wagner, Proceedings of IAEA Fusion Energy Conference, Geneva, Switzerland, 13–18 October 2008, Paper No. IT/P6-26.
- <sup>5</sup>A. Campos and C. H. Skinner, *J. Undergraduate Research* **IX**, 30 (2009), available from [http://www.scied.science.doe.gov/scied/JUR\\_v9/default.htm](http://www.scied.science.doe.gov/scied/JUR_v9/default.htm).
- <sup>6</sup>G. Counsell, A. P. C. de Vere, N. St. J. Braithwaite, S. Hillier, and P. Bjorkman, *Rev. Sci. Instrum.* **77**, 093501 (2006).
- <sup>7</sup>S. I. Krasheninnikov, A. Yu. Pigarov, R. D. Smirnov, M. Rosenberg, Y. Tanaka, D. J. Benson, T. K. Soboleva, T. D. Rognien, D. A. Mendis, B. D. Bray, D. L. Rudakov, J. H. Yu, W. P. West, A. L. Roquemore, C. H. Skinner, J. L. Terry, B. Lipschultz, A. Bader, R. S. Granetz, C. S. Pitcher, N. Ohno, S. Takamura, S. Masuzaki, N. Ashikawa, M. Shiratani, M. Tokitani, R. Kumazawa, N. Asakura, T. Nakano, A. M. Litnovsky, R. Maqueda, and the LHD Experimental Group, *Plasma Phys. Controlled Fusion* **50**, 124054 (2008).
- <sup>8</sup>C. J. Lasnier, S. L. Allen, J. A. Boedo, M. Groth, N. H. Brooks, A. McLean, B. LaBombard, C. H. Skinner, D. L. Rudakov, W. P. West, and C. P. C. Wong, *Fusion Sci. Technol.* **53**, 640 (2008).
- <sup>9</sup>D. L. Rudakov, J. H. Yu, J. A. Boedo, E. M. Hollmann, S. I. Krasheninnikov, R. A. Moyer, S. H. Muller, A. Yu. Pigarov, M. Rosenberg, R. D. Smirnov, W. P. West, R. L. Boivin, B. D. Bray, N. H. Brooks, A. W. Hyatt, C. P. C. Wong, A. L. Roquemore, C. H. Skinner, W. M. Solomon, S. Ratynskaia, M. E. Fenstermacher, M. Groth, C. J. Lasnier, A. G. McLean, and P. C. Stangeby, *Rev. Sci. Instrum.* **79**, 10F303 (2008).
- <sup>10</sup>A. Bader, C. H. Skinner, A. L. Roquemore, and S. Langish, *Rev. Sci. Instrum.* **75**, 370 (2004).
- <sup>11</sup>C. H. Skinner, A. L. Roquemore, A. Bader, and W. R. Wampler, *Rev. Sci. Instrum.* **75**, 4213 (2004).
- <sup>12</sup>C. Voinier, C. H. Skinner, and A. L. Roquemore, *J. Nucl. Mater.* **346**, 266 (2005).
- <sup>13</sup>C. V. Parker, C. H. Skinner, and A. L. Roquemore, *J. Nucl. Mater.* **363–365**, 1461 (2007).
- <sup>14</sup>C. H. Skinner, R. Hensley, and A. L. Roquemore, *J. Nucl. Mater.* **376**, 29 (2008).
- <sup>15</sup>D. P. Boyle, C. H. Skinner, and A. L. Roquemore, *J. Nucl. Mater.* **390–391**, 1086 (2009).
- <sup>16</sup>D. A. Gates, J. Ahn, J. Allain, R. Andre, R. Bastasz, M. Bell, R. Bell, E. Belova, J. Berkery, R. Betti, J. Bialek, T. Biewer, T. Bigelow, M. Bitter, J. Boedo, P. Bonoli, A. Boozer, D. Brennan, J. Breslau, D. Brower, C. Bush, J. Canik, G. Caravelli, M. Carter, J. Caughman, C. Chang, W. Choe, N. Crocker, D. Darrow, L. Delgado-Aparicio, S. Diem, D. D’Ippolito, C. Domier, W. Dorland, P. Efthimion, A. Ejiri, N. Ershov, T. Evans, E. Feibush, M. Fenstermacher, J. Ferron, M. Finkenthal, J. Foley, R. Frazin, E. Fredrickson, G. Fu, H. Funaba, S. Gerhardt, A. Glasser, N. Gorelenkov, L. Grisham, T. Hahn, R. Harvey, A. Hassanein, W. Heidbrink, K. Hill, J. Hillesheim, D. Hillis, Y. Hirooka, J. Hosea, B. Hu, D. Humphreys, T. Idehara, K. Indreshkumar, A. Ishida, F. Jaeger, T. Jarboe, S. Jardin, M. Jaworski, H. Ji, H. Jung, R. Kaita, J. Kallman, O. Katsuro-Hopkins, K. Kawahata, E. Kawamori, S. Kaye, C. Kessel, J. Kim, H. Kimura, E. Kolemen, S. Krasheninnikov, P. Krstic, S. Ku, S. Kubota, H. Kugel, R. La Haye, L. Lao, B. LeBlanc, W. Lee, K. Lee, J. Leuer, F. Levinton, Y. Liang, D. Liu, N. Luhmann, Jr., R. Maingi, R. Majeski, J. Manickam, D. Mansfield, R. Maqueda, E. Mazzucato, D. McCune, B. McGeehan, G. McKee, S. Medley, J. Menard, M. Menon, H. Meyer, D. Mikkelsen, G. Miloshevsky, O. Mitarai, D. Mueller, S. Mueller, T. Munsat, J. Myra, Y. Nagayama, B. Nelson, X. Nguyen, N. Nishino, M. Nishiura, R. Nygren, M. Ono, T. Osborne, D. Pacella, H. Park, J. Park, S. Paul, W. Peebles, B. Penafior, M. Peng, C. Phillips, A. Pigarov, M. Podesta, J. Preinhaelter, A. Ram, R. Raman, D. Rasmussen, A. Redd, H. Reimerdes, G. Rewoldt, P. Ross, C. Rowley, E. Ruskov, D. Russell, D. Ruzic, P. Ryan, S. Sabbagh, M. Schaffer, E. Schuster, S. Scott, K. Shaing, P. Sharpe, V. Shevchenko, K. Shinohara, V. Sizyuk, C. Skinner, A. Smirnov, D. Smith, S. Smith, P. Snyder, W. Solomon, A. Sontag, V. Soukhanovskii, T. Stoltzfus-Dueck, D. Stotler, T. Strait, B. Stratton, D. Stutman, R. Takahashi, Y. Takase, N. Tamura, X. Tang, G. Taylor, C. Taylor, C. Ticos, K. Tritz, D. Tsarouhas, A. Turndbull, G. Tynan, M. Ulrickson, M. Umansky, J. Urban, E. Uterberg, M. Walker, W. Wampler, J. Wang, W. Wang, A. Welander, J. Whaley, R. White, J. Wilgen, R. Wilson, K. Wong, J. Wright, Z. Xia, X. Xu, D. Youchison, G. Yu, H. Yuh, L. Zakharov, D. Zemlyanov, and S. Zweben, *Nucl. Fusion* **49**, 104016 (2009).
- <sup>17</sup>A. L. Roquemore, N. Nishino, C. H. Skinner, C. Bush, R. Kaita, R. Maqueda, W. Davis, A. Yu. Pigarov, and S. I. Krasheninnikov, *J. Nucl. Mater.* **363–365**, 222 (2007).
- <sup>18</sup>J. P. Sharpe, P. W. Humrickhouse, C. H. Skinner, the NSTX Team, T. Tanabe, K. Masaki, N. Miya, the JT-60U Team, and A. Sagara, *J. Nucl. Mater.* **337–339**, 1000 (2005).
- <sup>19</sup>Stabilized Metallic Lithium Powder from FMC Corporation (trade marked SLMP). Particle size is 44  $\mu\text{m}$  average diameter with a 40 nm coating of Li<sub>2</sub>CO<sub>3</sub>.
- <sup>20</sup>B. Rais and C. H. Skinner “Calibration of an electrostatic dust detector,” PPPL Report No. PPPL-4537, 2010.
- <sup>21</sup>D. K. Mansfield, A. L. Roquemore, H. Schneider, J. Timberlake, H. Kugel, M. G. Bell, and the NSTX Research Team, Proceedings of the 2nd NIFS-CRC International Symposium on Plasma-Surface Interactions NIFS, Toki, Gifu, Japan, 18–20 January 2010.